

Article

Ultrasonically Assisted Electrocoagulation Combined with Zeolite in Compost Wastewater Treatment

Sandra Svilović , Nediljka Vukojević Medvidović * , Ladislav Vrsalović , Senka Gudić  and Ana-Marija Mikulandra

Faculty of Chemistry and Technology, University of Split, Ruđer Bošković 35, 21000 Split, Croatia; sandra@ktf-split.hr (S.S.); ladislav@ktf-split.hr (L.V.); sgudic@ktf-split.hr (S.G.); anamarija.mikulandra@gmail.com (A.-M.M.)

* Correspondence: nvukojev@ktf-split.hr

Abstract: In this paper, the possibility of combining electrocoagulation (EC), ultrasound, and the addition of zeolite for wastewater treatment was investigated for the first time. The following combinations of hybrid processes were tested: electrocoagulation with zeolite (ECZ), simultaneous electrocoagulation with zeolite and ultrasound (ECZ+US), and two-stage electrocoagulation with zeolite and ultrasound (US+Z - EC), carried out with three different electrode materials. The results show that the simultaneous assistance of ultrasound in the ECZ leads to a lower increase in pH, while the temperature increase is higher. Regarding the COD, the assistance of ultrasound is only useful for Zn electrodes in the two-stage US+Z - EC, while the reduction in voltage consumption occurs for Fe and Al electrodes. Ultrasonic assistance caused more damage to the anodes, but anode consumption was reduced for Al and Zn electrodes. The total amount of zeolite that can be recovered is between 55–97%, and recovery is higher in systems with higher turbidity reduction. Good settling ability is only achieved with Al and Fe electrodes in simultaneous performance. Taguchi's orthogonal L9 array design was applied to analyze the effects of electrode material, process type, mixing speed, and time duration on COD decrease, settling velocity, electrode, and voltage consumption. The results show that the use of ultrasound does not contribute to the desired result and generally only has a favorable effect on voltage and electrode consumption, while it has no positive effect on settling ability or COD decrease. Furthermore, although longer times and higher mixing speeds negatively impact cost due to voltage and electrode consumption, it is advisable not to choose the shortest duration and lowest speed to obtain adequate wastewater treatment quality.

Keywords: triple combination; electrocoagulation; zeolite; ultrasound; compost wastewater



Citation: Svilović, S.; Vukojević Medvidović, N.; Vrsalović, L.; Gudić, S.; Mikulandra, A.-M. Ultrasonically Assisted Electrocoagulation Combined with Zeolite in Compost Wastewater Treatment. *Processes* **2024**, *12*, 951. <https://doi.org/10.3390/pr12050951>

Academic Editor: Maria Jose Martin de Vidales

Received: 28 March 2024

Revised: 28 April 2024

Accepted: 1 May 2024

Published: 8 May 2024



Copyright: © 2024 by the authors. Licensee MDPI, Basel, Switzerland. This article is an open access article distributed under the terms and conditions of the Creative Commons Attribution (CC BY) license (<https://creativecommons.org/licenses/by/4.0/>).

1. Introduction

Population growth, industrialization, and urbanization are leading to ever-increasing quantities of wastewater with a very complex composition. Therefore, there is a growing need for efficient wastewater treatment solutions that enable reuse and recycling [1]. This approach is in line with the principles of the circular economy, which is widely recognized as a model for sustainable development and the prevention of drinking water shortages in the future. Wastewater is no longer seen as waste, but as a resource [2]. In this context, many scientists are interested in developing integrated or combined treatment solutions based on combining two or more individual physical, chemical, or biological treatment processes [3]. In this paper, the coupling of ultrasound with electrocoagulation and zeolite as an integrated treatment solution was investigated for the first time.

Ultrasound is generally defined as a longitudinal wave with frequencies above 20 kHz. The application of ultrasound is simple, as it generally requires low investment costs and no addition of chemicals [4]. However, when it is applied for wastewater treatment, it is usually combined with other treatment processes to reduce energy consumption [5] and

enhance treatment efficiency [6,7]. There are several successful applications of technological solutions based on the use of ultrasound [8–11]. Sangave and Pandit (2004) [8] found that ultrasonic irradiation as a pre-treatment step followed by aerobic oxidation of distillery spentwash contributes to increasing initial rates of degradation by converting the organic molecules of the initial pollutant into simpler forms. Blume and Neis (2004) [9] investigated the application of low-frequency ultrasound (20 kHz) to improve the dewatering ability of digested sludge from a petrol plant and the reduction in the final moisture content of the sludge. They found that ultrasound as a pretreatment step in combination with ultraviolet irradiation of wastewater contributes to disinfection efficacy more than an order of magnitude higher. Yin et al. (2006) [10] found that the application of low-frequency ultrasound (20 kHz) improved the dewatering ability of digested sludge from a petrol plant and reduced the final moisture content of the sludge. Kyllönen et al. (2006) [11] found that ultrasound-based on-line cleaning performed at atmospheric pressure during an intermission pause is an efficient and gentle membrane-cleaning method in the membrane treatment of industrial wastewater.

Recently, some authors combined electrocoagulation with ultrasound for wastewater treatment [5,6,12]. Emerick et al. (2020) [12] coupled the electrocoagulation on Al or Al/Fe electrodes with ultrasound (EC+US) for the treatment of swine slaughterhouse wastewater. They found that the effluent was completely clarified after 15 min of electrocoagulation with ultrasound. The average color removal was 95%, and the turbidity removal was 97%. Alnaimi et al. (2020) [13] combined ultrasound and electrocoagulation with four Al electrodes for effluents of concrete plants, achieving an enhanced chemical oxygen demand (COD) decrease compared to EC alone (68.14 vs. 87.8% of COD decrease). Zhang et al. (2020) [7] found that ultrasound-assisted electrochemical treatment with the addition of fly ash-loaded titanium $\text{TiO}_2\text{-Fe}^{3+}$ particles was more efficient for phenolic wastewater compared to ultrasonic treatment alone, Fenton reagent alone, and ultrasound combined with H_2O_2 treatment.

The combined EC+US achieves a synergistic effect of coagulation, flocculation, and flotation with ultrasonic cavitation. Sound waves create pressure fluctuations that lead to the formation, growth, and implosion of microbubbles [6,12,14]. According to Wang et al. (2023) [5], the collapse of a microbubble generates shock waves, micro jets, hydroxyl radicals ($\cdot\text{OH}$), and high pressure, which can further produce mechanical, chemical, and thermal effects, resulting in increased mineralization of organic pollutants. According to Elazzouzi et al. (2017) [15], electrocoagulation–flotation processes and electrocoagulation–flotation processes with ultrasound can produce monomeric and polymeric aluminum hydroxide complexes which affect the efficiency of the process.

On the other side, the ultrasound was also coupled with zeolite in order to increase the zeolite binding capacity. Zielinski et al. (2015) [16] found that the sorption capacity of zeolite to remove ammonia can be improved by treatment with 35 kHz ultrasound for 15, 30, 45, 60, and 90 min. They obtained increased efficiency of ammonia removal by 14%, while the rate of ammonia removal was 30% higher than with natural zeolite without ultrasound treatment. Jahani et al. (2023) [17] found that modification of natural zeolite was efficiently performed by ultrasonic-assisted chemicals (NaOH, FeCl_3 , and HCl), and enhanced ammonium removal from wastewater was achieved. Znak et al. (2021) [18] found that natural clinoptilolite can be efficiently modified with silver ions using ultrasound. They also concluded that the use of ultrasound ensures the desorption of air from zeolite particles and accelerates the diffusion of silver ions and subsequent ion exchange. Erten-Kaya and Cakicioglu-Ozkan (2012) [19] found that the application of ultrasound enhances the replacement of Na^+ ions with Li^+ , Ca^{2+} , and Ce^{3+} ions in the extra-framework of NaX zeolite by up to 76%, 72%, and 66%, respectively. They concluded that ultrasound acts as a co-driven force for the concentration of counter ions in the solution due to the cavitation effect.

Based on all previously mentioned studies, it is evident that ultrasound assistance may enhance electrocoagulation and increase zeolite capacity. Therefore, the goal of this re-

search is to investigate how the addition of zeolite and the use of ultrasound could enhance electrocoagulation efficiency. As far as we know, this triple combination (electrocoagulation, zeolite, and ultrasound) as a wastewater hybrid treatment process was investigated for the first time. Three different combinations of hybrid processes were tested: electrocoagulation with zeolite, simultaneous electrocoagulation with zeolite and ultrasound, and two-stage electrocoagulation with zeolite and ultrasound, performed with three different electrode materials. The comparison includes the analysis of physical–chemical parameters in solution, electrode consumption and surface electrode change, mass of the collected sludge, and settling ability of the suspension. In addition, Taguchi optimization was applied to analyze the effects of the electrode material, process type, mixing speed, and time duration on COD decrease, settling velocity, and electrode and voltage consumption. Based on the obtained results, guidelines regarding the opportunities and challenges of ultrasound coupled with electrocoagulation and zeolite as wastewater treatment solutions will be given.

2. Materials and Methods

Compost wastewater: prepared from Agro compost and characterized by a pH of 4.72, an electrical conductivity of 1.958 mS/cm, a turbidity of 258.67 NTU, a temperature of 23.9 °C, a chemical oxygen demand (COD) of 864.93 mg O₂/L, and a total solids (TS) content of 1615 mg/L, as determined according to the Standard Water and Wastewater Testing Methods [20].

Electrodes: aluminum alloy AA2007 (Al = 92.58%, Cu = 3.84%), commercial zinc sacrificial anodes (Zn = 99.31–99.76%, Al = 0.1–0.5%), and carbon steel (Fe = 98.27%, Cu = 1.17%) [21]. The composition and preparation of the electrodes has been described previously [21,22].

Synthetic zeolite (SZ): purchased from Alfa Aesar. The zeolite was crushed and sieved, and a size < 40 µm was used in this study.

The treatment of compost wastewater with hybrid processes: Three different combination of hybrid processes were tested: (a) electrocoagulation coupled with zeolite (ECZ); (b) simultaneous electrocoagulation coupled with zeolite and ultrasound (ECZ+US); and (c) two-stage electrocoagulation coupled with zeolite and ultrasound (US+Z - EC) performed sequentially, i.e., in two steps, whereby zeolite was combined with ultrasound (US+Z) for 10 min in the first step and electrocoagulation (EC) was carried out in the second step. The performance of each hybrid process is given in Figure 1.

In the first part of the study, all hybrid processes were carried out in an electrochemical cell with 500 mL of initial wastewater solution and with a pair of immersed electrodes (Al, Fe, or Zn) at a distance of 3 cm at a mixing speed of 150 rpm, a contact time of 30 min, and a current density of 0.0182 A/cm², while the addition of synthetic zeolite and NaCl electrolyte (p.a., Merk, Darmstad, Germany) was 15 g/L and 0.5 g/L, respectively. Current was obtained using laboratory power supply Wanptek DPS605U, China, with a precise current and potential adjustment. Hybrid processes of electrocoagulation with zeolite and ultrasound were carried out by immersing the electrochemical cell in an ultrasonic bath, Asonic Pro 30, with an ultrasonic frequency of 40 kHz and a tank capacity of 2.8 L. The tank was filled with distilled water.

The following physical–chemical parameters were analyzed to compare each process: pH value (pH meter, Seven Multi, Mettler Toledo), temperature in the electrochemical cell and in the ultrasonic bath (digital thermometer Testo 720), COD (standard dichromate method), turbidity (turbidimeter, Welp), total mass of the electro-generated sludge and the saturated zeolite (by weighing method), as well as voltage consumption (displayed on the power supply's LCD screen). The experiments' marks (process and electrode type) and the results obtained are compared in Table 2 (see Section 4).

In addition, the changes in electrode mass were analyzed using the weighing method, while the changes on the electrode surface were examined using a light microscope (MXFMS-BD, Ningbo Sunny Instruments Co., Ningbo, China) with a 100× magnification in combination with a Canon EOS 1300D digital camera.

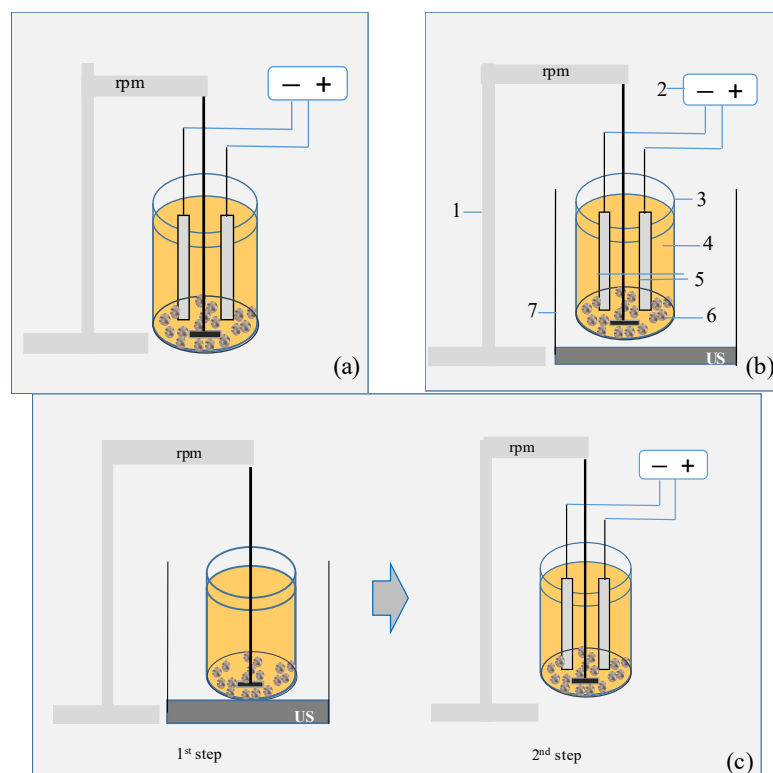


Figure 1. Schematic presentation of the performance of hybrid processes: (a) electrocoagulation coupled with zeolite (ECZ); (b) simultaneous electrocoagulation coupled with zeolite and ultrasound (ECZ+US); and (c) two-stage electrocoagulation coupled with zeolite and ultrasound (US+Z - EC) performed sequentially, i.e., in two steps, where in the first step zeolite was combined with ultrasound (US+Z) for 10 min and in the second step electrocoagulation (EC) was performed. Note: 1—laboratory stirrer, 2—DC power supply, 3—glass beaker, 4—compost wastewater, 5—pair of electrodes, 6—synthetic zeolite, 7—ultrasonic bath.

The settling ability of the suspensions after performing the hybrid processes was analyzed using the Kynch standard batch-settling test [23]. The principle of the Kynch method is based on the sedimentation of the suspension in a graduated cylinder (beaker), with reading of the height of the precipitated sediment column at certain time intervals. In addition, the settling potential was also measured as the potential difference between two stainless steel electrodes (areas of 2 cm²) placed between the top and bottom of the cylinder during the Kynch test. The settling potential was measured with a voltmeter (Intelligent Digital Multimeter UT71) and resulted from the fact that suspended particles leave a solvated sphere with the opposite charge when they move under the influence of gravity.

3. Optimization by Taguchi

In the second part of the study, the experiments were planned according to Taguchi's L9 orthogonal array design. These experiments were also performed with an electrode distance of 3 cm, a current density of 0.0182 A/cm², and with the addition of synthetic zeolite and NaCl electrolyte at 15 g/L and 0.5 g/L, respectively. The effects of electrode material (Fe, Al, Zn), process type (ECZ, ECZ+US, and US+Z - EC), mixing speed (50, 150, and 250 rpm) and experiment duration (10, 20, and 30 min) on the COD decrease, settling velocity, electrode consumption, and voltage consumption were investigated. As can be seen, each controllable factor had three test levels (Table 1).

Table 1. Design of the experiments using Taguchi L9.

Exp. Mark	Exp. Condition	Electrode Material (M)	Process Type (PT)	Mixing Speed, rpm (N)	Duration Time, min (t)
A1	ECZ, Fe, 50 rpm, 10 min	Fe	ECZ	50	10
A2	ECZ+US, Fe, 150 rpm, 20 min	Fe	ECZ+US	150	20
A3	US+Z - EC, Fe, 250 rpm, 30 min	Fe	US+Z - EC	250	30
A4	ECZ, Al, 150 rpm, 30 min	Al	ECZ	150	30
A5	ECZ+US, Al, 250 rpm, 10 min	Al	ECZ+US	250	10
A6	US+Z - EC, Al, 50 rpm, 20 min	Al	US+Z - EC	50	20
A7	ECZ, Zn, 250 rpm, 20 min	Zn	ECZ	250	20
A8	ECZ+US, Zn, 50 rpm, 30 min	Zn	ECZ+US	50	30
A9	US+Z - EC, Zn, 150 rpm, 10 min	Zn	US+Z - EC	150	10

Considering that the aim of this study was to determine the optimum conditions for the highest COD decrease and settling velocities, as well as the lowest electrode and voltage consumption, the larger-the-better and smaller-the-better quality characteristics were chosen. Equations (1) and (2) represent these quality characteristics.

$$S/N_{LB} = -10 \log \frac{\sum_{i=1}^n \frac{1}{y_i^2}}{n} \quad (1)$$

$$S/N_{SB} = -10 \log \frac{\sum_{i=1}^n y_i^2}{n} \quad (2)$$

where S/N is the signal-to-noise ratio, LB is the larger-the-better subscript, SB is the smaller-the-better superscript, n is the number of repeats under identical conditions, and y is the value determined from the experiment [21]. In addition to the S/N_{LB} and S/N_{SB} , for a more effective process evaluation, the S/N ratio, percentage of contribution (pC), sum of squares (SS), mean square (MS), range, and rank were calculated for each controllable factor.

4. Results and Discussion

During the EC process, the anode (Al, Zn, Fe) acts as a sacrificial electrode and dissolves (corrodes), while the metal ions enter the solution and undergo a process of spontaneous hydrolysis (colloidal particles with different positive charges are formed and the area around the anode becomes acidic). At the same time, a reaction of hydrogen excretion takes place at the cathode with the formation of hydroxide ions (with an increase in alkalinity). The hydrolysis products can react with OH^- ions and finally transform into amorphous metal hydroxide and/or polyhydroxide (often large Me–O–Me–OH networks) in the solution mass following complex precipitation kinetics [24,25]. The way in which the metal ions form during the EC process is generally explained by two interrelated steps: the neutralization of positively charged metal colloids and incorporation of impurities into the precipitate of amorphous hydroxide (“sweep flocculation”). The relative importance of these mechanisms depends strongly on the pH and the dose of the coagulant (the type of anode material, i.e., the rate of its dissolution) [26,27]. Zeolite acts as an adsorbent and ion-exchanger, but also contributes to reducing electrode passivation [22]. In the following, the effects of simultaneous and two-stage ultrasonic assistance with three different electrodes on the efficiency of each process type, the electrode wear, and the settling ability are investigated.

4.1. Analysis of Physical–Chemical Parameters in Solution

In the first part of the discussion, the results of the physical–chemical parameters of the wastewater during and after treatment are presented.

In all ECZ processes, there was a sudden increase in pH in the first 5 min with Al and Zn electrodes to 9.85 and 11.83, respectively, after which the pH did not change significantly

(Figure 2). The final pH values were 10.01 and 13.35 for the Al and Zn electrodes. In the case of ECZ with the Fe electrode, the pH value continuously increased up to a final value of 12.07. Thus, the highest pH increase order followed the order Zn > Fe > Al, which is consistent with previous results [21].

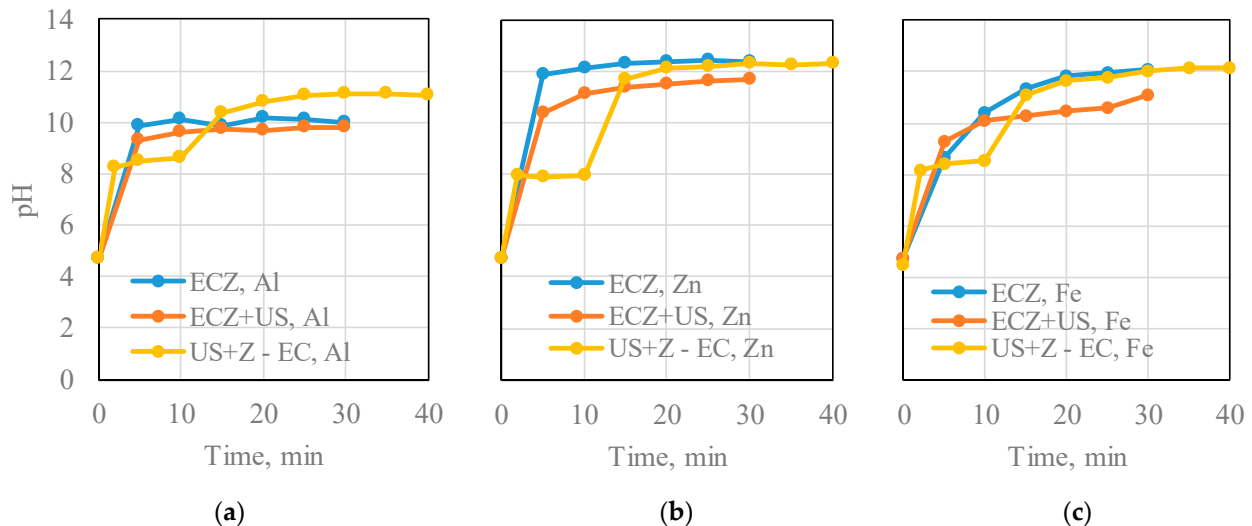


Figure 2. Evolution of the pH value during each hybrid process carried out with electrodes made of: (a) Al, (b) Zn, and (c) Fe alloys.

With simultaneous ECZ+US, a similar behavior of pH change was obtained, but the pH values were slightly lower. This indicates that the simultaneous assistance of ultrasound in ECZ causes a lower increase in pH. However, these differences were quite small for Al electrodes, whereas the pH difference was more pronounced for Zn and Fe electrodes.

In the two-stage ECZ with ultrasound (UC+Z - EC), the pH change curves showed similar behavior. In the first stage, zeolite was combined with ultrasound (US+Z) for 10 min, resulting in an increase in pH to 7.97–8.60, while in the second stage, when electrocoagulation (EC) was performed, a greater increase in pH was observed. The final pH was almost the same as when Zn and Fe electrodes were used in ECZ. However, when Al electrodes were used, the final pH was higher than with ECZ, reaching 11.05. It is interesting to note that the final increase in pH occurred in the same order in all hybrid process types: Zn > Fe > Al.

According to the Pourbaix diagrams for Al, Zn, and Fe [28–32], the change in pH influences the formation of monomeric and polymeric hydroxocomplexes with higher or lower coagulation/flocculation abilities, and, thus, will influence the final COD and turbidity (see Table 2).

Table 2. Parameters results measured for each hybrid process.

Exp Mark	T, °C	T _{bath} , °C	Turbidity _{fin} , NTU	Turbidity Decrease, %	COD _{fin} , mg O ₂ /L	COD Decrease, %	Mass (EC Sludge + Saturated Zeolite), g/L	Voltage, V
ECZ, Al	32.8	-	23.73	90.82	62.87	92.73	16.4454	25.22
ECZ+US, Al	44.2	38.0	29.70	88.52	145.71	87.19	15.5012	30.38
US+Z - EC, Al	33.3	29.2	63.70	75.37	137.72	84.08	13.6756	14.87
ECZ, Zn	34.5	-	65.47	74.69	201.60	76.69	12.9348	20.96
ECZ+US, Zn	45.1	39.7	267.00	-3.22	280.44	67.58	10.0208	28.33
US+Z - EC, Zn	37.8	25.5	18.24	92.95	147.75	82.92	12.7308	25.24
ECZ, Fe	28.3	-	8.42	96.74	77.84	91.00	16.2690	20.33
ECZ+US, Fe	36.4	35.7	49.65	80.81	95.81	88.92	15.1626	16.82
US+Z - EC, Fe	31.1	29.6	241.50	6.64	171.66	80.15	12.3272	17.74

The increase in temperature is visible in all hybrid combinations. The largest increase was recorded with the simultaneous ECZ+US, followed by the two-stage US+Z - EC, and the smallest with the application of ECZ. Obviously, ultrasound assistance contributed to the increase in temperature. Although the temperature rise was lower in the two-stage US+Z - EC due to the shorter exposure time to the US, the temperature increase in the ultrasonic bath was lower compared to the EC reactor. Looking at the type of electrode material, the largest temperature increases were observed for the Zn electrode, followed by the Al electrode, and the smallest temperature increases were observed for the Fe electrodes.

The turbidity values fluctuated. The greatest reduction in turbidity was achieved with the ECZ process with Al and Fe electrodes, which amounted to 90.82% and 96.74%, respectively. Ultrasound assistance reduced the percentage of turbidity decrease for Al electrodes and amounted to 88.52% with simultaneous ECZ+US and 75.37% with two-stage US+Z - EC. For Fe electrodes, the turbidity reduction was lower and amounted to 80.81% with ECZ+US, while only 6.64% was achieved with two-stage US+Z - EC. In the case of Zn electrodes, the greatest reduction in turbidity was recorded with two-stage US+Z - EC at 92.95%, followed by single ECZ at 74.69%, while with simultaneous ECZ+US, there was even an increase in turbidity compared to the initial value.

The COD decrease fluctuated in a range of 67.58–92.73%. In general, the highest values were achieved with the Al electrode (84.08–92.73%), followed by Fe (80.15–91.00%) and the Zn electrode (67.58–82.92). However, ultrasonic assistance lowered the COD decrease for Al and Fe electrodes, while a slight increase was observed only for the Zn electrode in the two-stage US+Z - EC. According to Sangave and Pandit (2004) [8], ultrasonic waves contribute to the restructuring of molecules present in wastewater rather than their mineralization. Asgaharian et al. (2017) [33] applied electrocoagulation and ultrasound for the removal of humic acid (HA) from wastewater, considering different electrode material combinations (platinum, graphite, and aluminum electrodes), pH, time, voltage, temperature, and electrolyte concentration. They also found that the simultaneous application of ultrasound and electrocoagulation drastically reduced the removal efficiency.

The voltage consumption values also fluctuated with each hybrid process. In the hybrid system with Al electrodes, higher values for voltage consumption were achieved with simultaneous ECZ+US and ECZ compared to two-stage US+Z - EC. In the hybrid system with Zn electrodes, higher values for voltage consumption were achieved with simultaneous ECZ+US and two-stage US+Z - EC compared to ECZ. However, the hybrid system with Fe electrodes behaved in the opposite way, i.e., lower voltage consumption values were achieved with simultaneous ECZ+US and two-stage US+Z - EC compared to ECZ.

Based on the final values obtained for the parameters analyzed after applying each hybrid process (see Figure 1 and Table 2), it can be seen that the final pH value exceeded the limits prescribed by the Croatian regulation for discharge into the sewage system (pH = 6.5–9.5) [34]. Therefore, an additional adjustment was required. With the exception of the ECZ with the Fe electrode, all hybrid types also required a temperature adjustment before discharge into the natural receiving water (30 °C), while ECZ+US with Al and Zn required a temperature adjustment before discharge into sewage system (40 °C) in order to avoid thermal pollution. The situation was similar to the values of the turbidity parameters, even if the limit values were not prescribed in the Croatian regulation. The discharge of wastewater with high turbidity can affect the process of photosynthesis in water systems and the reduction in oxygen content. Regarding COD, the final values for most of the hybrid process were slightly above the limits for discharge into the natural recipient (125 mg O₂/L), while the values for ECZ with Al and Fe and ECZ+US with Fe were within the range.

4.2. Analysis of Electrode Consumption and Surface Electrodes Change

Anode and cathode electrode consumptions, determined by weighing methods, are compared in Figure 3.

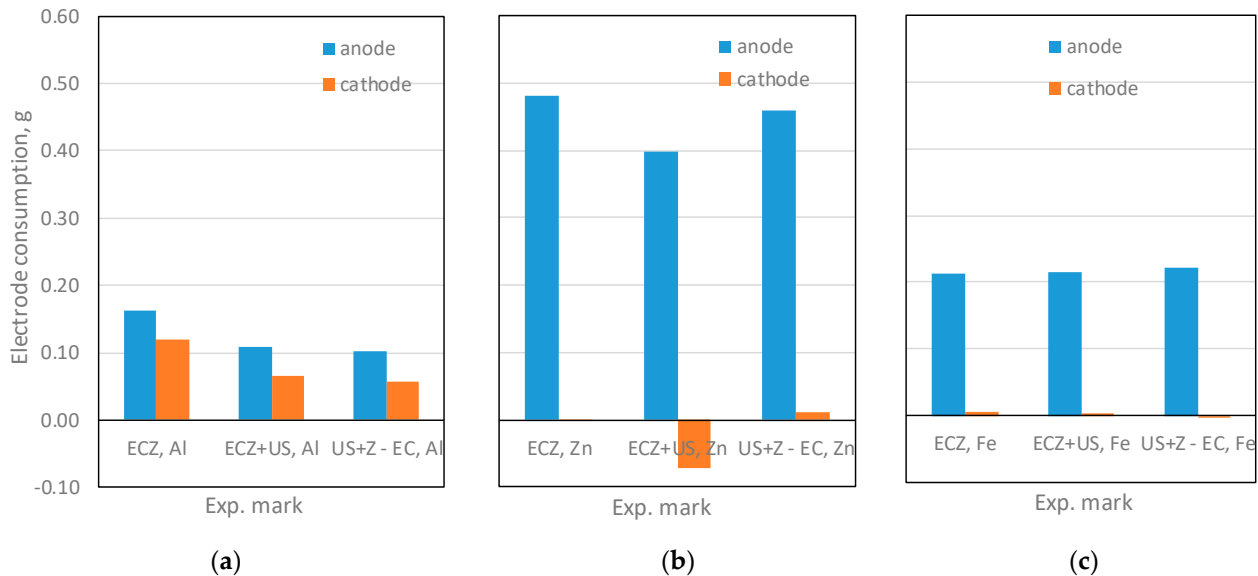


Figure 3. Electrode consumption after each hybrid processes performed with electrodes made of (a) Al; (b) Zn; (c) Fe alloys.

Anode consumption dominated compared to cathode consumption. The highest anode consumption was achieved with Zn electrodes, followed by Fe, and the lowest with Al electrodes. It can also be seen that ultrasonic assistance reduced anode consumption with Al and Zn electrodes, while it caused a slight increase in anode consumption with Fe electrodes. The consumption of cathodes varied (increases or decreases) depending on the type of hybrid process and electrode material, but in general, the consumption of aluminum cathodes was the highest.

The changes on the surfaces of the electrodes were analyzed using an optical microscope with $100\times$ magnification, and the results are compared in Figure 4.

In the hybrid ECZ process with Al electrodes, damages to the anode and cathode surfaces were almost equal, which was consistent with the electrode consumption. Ultrasonic assistance generated greater damage to the anodes, which was especially noticeable with simultaneous ECZ+US. According to Wang et al. (2023) [5], the cavitation bubbles generated as a result of the cavitation effect can increase the active surface area of solid surface materials through the pitting effect. According to Zang et al. (2020) [7], the micro jets and shock waves contributed to the reduction of the thickness of the diffusion layer on the surface of the electrode. The micro-jet and shock waves caused by ultrasonic cavitation could cause macroturbulence of the liquid medium, which favors continuous renewal on the electrode surface [35].

De Moraes and Brett (2002) [36] investigated the influence of power ultrasound on the corrosion of aluminum and steel in a chloride-containing medium and found that ultrasound led to the destruction of the oxide film in aluminum, while in steel, its effect manifested itself in the removal of corrosion products and increased mass transport of the solution, resulting in higher corrosion attack.

In the hybrid systems with Zn electrodes, the anode was also more damaged than the cathode. Ultrasonic assistance resulted in the anode being damaged even more severely. This can be explained by the fact that the Zn anode was exposed to maximum mass transfer in the ultrasonic bath, and the ultrasound led to activation of the Zn oxidation reaction, which was found by Doche et al. (2003) [37]. They found that the corrosion of Zn in salt solution was significantly higher with ultrasonic assistance [37].

In the hybrid systems with Fe electrodes, intensive corrosion damage could be seen on the surfaces of the anodes and cathodes. Ultrasonic assistance resulted in both electrodes being more severely damaged, and the damage was more pronounced in a two-stage

hybrid process (US+Z - EC). Cathode damage indicates pitting corrosion, while surface damage on Fe anodes indicates uniform anodic dissolution and localized corrosion.

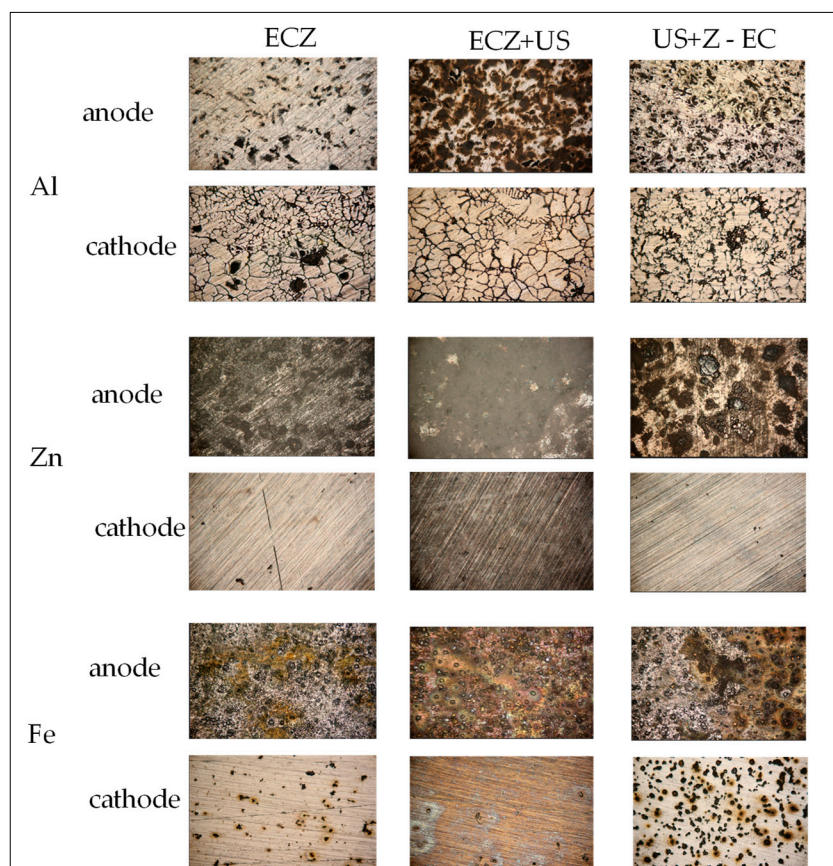


Figure 4. The changes in electrodes' surfaces, analyzed by a light microscope with 100× magnification.

4.3. Comparison of the Mass of Collected Sludge and Settling Ability of Suspension

The mass of EC sludge and saturated zeolite collected after experiments are compared in Table 2. Previous studies have shown that 0.1–1.75 g/L of EC sludge is collected during the EC process, depending on the experimental conditions [38]. In this study, in each hybrid process, an amount of 15 g/L of synthetic zeolite with a particle size < 40 μm was used, while the mass of EC sludge and saturated zeolite collected after each hybrid process varied in the range of 10.0218–16.4454 g/L, depending on the type of hybrid process and electrode material. This indicates that the total amount of zeolite that can be regenerated ranges from 55 to 97%. Additionally, the total amount of zeolite that could be regenerated was higher in the hybrid system, where better turbidity reduction was achieved, and vice versa.

The settling ability of the suspensions and the sedimentation potential after application of the hybrid processes are compared in Figure 5.

In a hybrid system with Al electrodes, good settling ability was achieved with ECZ and simultaneous ECZ+US (both settling curves were steep), while it was quite poor with the two-stage US+Z - EC (the settling curve was flattened). A similar behavior was observed when using Fe electrodes, indicating that the settling velocities were slightly slower, and the sediment layer was larger in all hybrid systems. However, in a hybrid system with Zn electrodes, poor settling performance was achieved in all three hybrid processes.

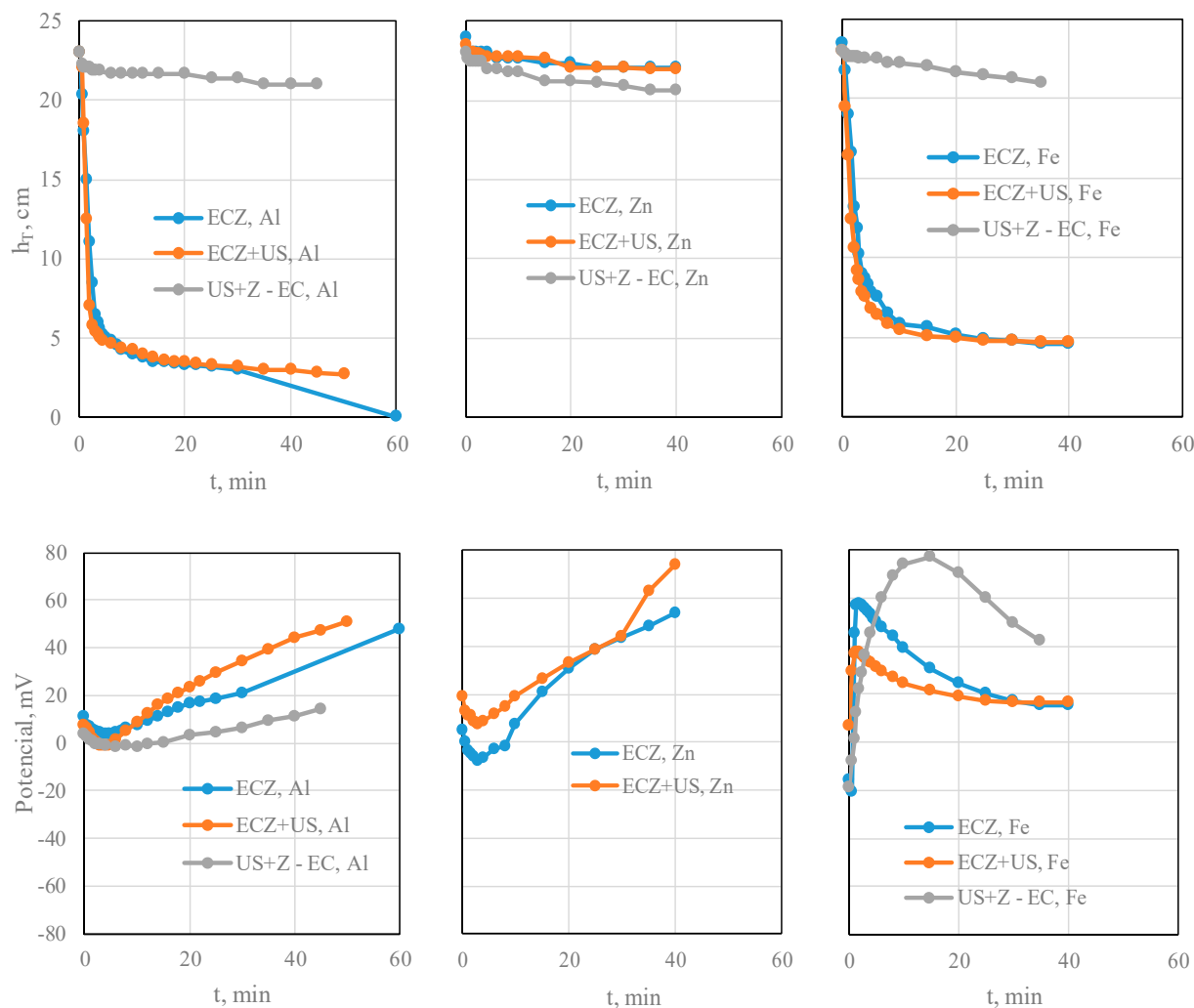


Figure 5. Comparison of the settling ability of the suspensions and the potential differences during settling after the implementation of the hybrid processes.

The high settling abilities when using Al and Fe electrodes in ECZ and ECZ+US systems resulted from a favorably dosed amount of metal ions (approx. 0.2 g with corresponding dissolution of the electrodes, Figure 3), which were subject to hydrolysis and subsequent coagulation and flocculation. In fact, this amount of metal ions in the observed systems was sufficient to overcome the attractive forces that led to the consolidation of the particles (leaving the range of colloidal dimensions), which facilitated settling ability. This was subsequently confirmed by a greater sludge mass and lower COD, as well as the turbidity of the treated water. The slightly better settling ability of Al electrodes compared to Fe electrodes was also supported by the higher oxidation state of the formed ions (Al^{3+} compared to Fe^{2+}), which increased the attractive forces and facilitated the formation of metal hydroxide and/or polyhydroxide and the deposition of colloidal particles. The consequence of poor settling and other characteristics in water treatment in a two-stage hybrid process is, most likely, that the first, i.e., the US stage, prevents the association of particles and their subsequent sedimentation.

The poor settling ability of hybrid systems with Zn electrodes was influenced by two factors. The first was the significant dissolution of the anode and the formation of a large amount of coagulant (i.e., Zn^{2+} ions). Coalescence of the particles was prevented by the electrostatic repulsive forces between the particles (equal charge in the outer parts of the double layer). Another reason for the poor settling performance in these systems was the high pH of the solution (11–12), which was reached very quickly (after only 5–10 min)

during the EC process (Figure 3). According to the Pourbaix diagrams, the Zn dissolved at these pH values in the form of zincate ions (ZnO_2^-), which, as complex ions, prevent the formation of hydroxides, coagulation, and, thus, precipitation [30].

By placing two stainless steel electrodes (same surfaces) between the top and bottom of the cylinder during settling, a certain potential difference was observed, caused by the suspended particles leaving a solvated sphere with the opposite charge as they moved under the influence of gravity. In this way, the tendency to separate the surface charge of the particles and the charge in the diffuse part of the double layer was expressed, which generated the corresponding electric field. This type of movement of the particle disturbed the equilibrium symmetry of the double layer of the particle, and the moving particle had a dipole character. The sum of the dipole effects of all moving particles represented the sedimentation potential, which, according to the literature [39], is directly proportional to the zeta potential (charge density in the diffuse part of the double layer) and the volume fraction of the particles and inversely proportional to the specific conductivity of the solution.

Figure 5 shows that the sedimentation potential was almost zero for all hybrid systems at the beginning of the measurement, and assumed positive values over time. According to H. Hirakawa's measurements [40], the sedimentation potential has a positive value when the molecular mass of the cation is greater than that of the anion, and it increases with the use of ultrasound during deposition (which is not always the case in this work, but the experimental conditions are also different). The dynamics of the changes in sedimentation potential are complex and depend on the material used and the hybrid cleaning method applied. In general, it can be said that the lower the thickness of the sedimentation layer in which the flocs are connected by stronger bonds, the higher the sedimentation potential. However, further measurements are required in order to better understand the results.

4.4. Taguchi Optimization

The experimental results from the Taguchi-planned studies, as well as the average S/N_{LB} or S/N_{SB} , depending on the factor analyzed, are presented in Table 3.

Table 3. Results of the experimental part of Taguchi design, and S/N_{LB} and S/N_{SB} ratios.

Exp. Mark	COD Decrease, %	S/N_{LB} for COD Decrease	Settling Velocity, cm/min	S/N_{LB} for Settling Rate	Voltage, V	S/N_{SB} for Voltage	Electrodes Mass Consumed, g	S/N_{SB} for Electrodes Mass Consumed
A1	78.57	37.905	0.096	-20.355	18.02	-25.115	0.0691	23.210
A2	87.34	38.824	1.300	2.279	17.64	-24.930	0.1752	15.129
A3	77.32	37.766	0.086	-21.310	18.79	-25.479	0.2021	13.889
A4	86.50	38.740	1.660	4.402	15.67	-23.901	0.1567	16.097
A5	74.14	37.401	0.080	-21.938	24.10	-27.640	0.0561	25.021
A6	79.12	37.966	0.060	-24.437	24.39	-27.744	0.1439	16.839
A7	75.32	37.538	0.100	-20.000	27.24	-28.704	0.3851	8.289
A8	68.64	36.732	0.080	-21.938	20.44	-26.209	0.4373	7.184
A9	66.88	36.506	0.090	-20.915	11.70	-21.364	0.1722	15.280

In addition to calculating the S/N ratio of each factor, the sum of squares (SS), the mean square (MF), the percentage of contribution (pC), and the range were also calculated. The contribution of these values lies in evaluating the relevance of the tested factors to the desired results of the process. The formula for the computation methods is given elsewhere [41]. The investigation of the optimum values of the parameters used shows (Table 4) that the maximum COD decrease should be achieved in the ECZ process with Fe electrodes at a mixing speed of 150 rpm and a duration of 20 min. The fastest settling should also be achieved in the ECZ process with Fe electrodes at a mixing speed of 150 rpm, but after 30 min. In terms of voltage consumption, the lowest values should, again, be achieved with Fe electrodes and at 150 rpm. In this optimization, however, the best process is the two-stage US+Z - EC process with the shortest duration. The lowest electrode consumption

should be achieved at the lowest mixing speed and ECZ process duration. However, as also found in previous studies, the electrode wears most slowly when is made of Al [38].

Table 4. Response table for S/N ratios and contribution of each factor.

Factor	COD Decrease				Settling Velocity			
	M	PT	N, rpm	t, min	M	PT	N, rpm	t, min
Level 1	38.17	38.06	37.53	37.27	−13.129	−11.984	−22.243	−21.069
Level 2	38.04	37.65	38.02	38.11	−13.991	−13.866	−4.746	−14.053
Level 3	36.96	37.41	37.57	37.75	−20.951	−22.221	−21.083	−12.949
Range	1.24	0.65	0.49	0.84	7.823	10.237	17.499	8.121
DoF	2	2	2	2	2	2	2	2
SS	2.79	0.65	0.45	1.06	110.4	178.1	574.5	116.4
MS	1.39	0.32	0.22	0.53	55.19	89.07	287.24	58.20
pC, %	56.40	13.06	9.06	21.48	11.27	18.19	58.66	11.88
Rank	1	3	4	2	4	2	1	3

Factor	Voltage consumption				Electrode mass consumed			
	M	PT	N, rpm	t, min	M	PT	N, rpm	t, min
Level 1	−25.17	−25.91	−26.36	−24.71	17.41	15.87	15.74	21.17
Level 2	−26.43	−26.26	−23.40	−27.13	19.32	15.78	15.50	13.42
Level 3	−25.43	−24.86	−27.27	−25.20	10.25	15.34	15.73	12.39
Range	1.25	1.40	3.88	2.42	9.07	0.53	0.24	8.78
DoF	2	2	2	2	2	2	2	2
SS	2.64	3.17	24.62	9.82	137.14	0.49	0.11	138.22
MS	1.32	1.59	12.31	4.91	68.57	0.25	0.06	69.11
pC, %	6.56	7.88	61.16	24.40	49.70	0.18	0.04	50.09
Rank	4	3	1	2	2	3	4	1

DoF—degree of freedom; SS—sum of square; MS—mean of square; pC—percentage of contribution; bold value (level) = optimal.

Although it is not possible to select the same factor levels for the best result for all four responses, certain common findings can be made, which, when combined with the results of the percentage contribution of each factor, can lead to a conclusion.

Regarding the process type, the best outcome is obtained when ECZ is selected. Ultrasonic assistance generally does not contribute to the desired result. Stirring the solution homogenizes the reaction mixture and accelerates ion mobility. Increasing the stirring speed to a certain degree improves the COD removal efficiency, settling rate, and voltage consumption if the selected stirring speed does not exceed the value at which the flocs begin to collapse [42]. In this study, the optimum value was 150 rpm.

As might be predicted, increasing the mixing speed and reaction time had a negative effect on electrode consumption. The longer the process lasted, the more the electrode dissolved, and the protective hydroxide interface surrounding the electrode was probably partially removed by the vigorous mixing. Although the process duration, as opposed to the mixing speed, had a significant influence on the consumption of the electrode, the maximum permissible limit for the discharge of wastewater into water bodies must be taken into account when selecting the process duration. The selection of the electrode material appears to be difficult, as the material is an important factor for both COD removal (Fe, pC = 56%) and electrode consumption (Al, 49%). However, a detailed analysis of the results in Table 3 shows that the high influence of the material on COD removal was due to the use of the Zn electrode, and that high COD removal values could also be achieved with the Al electrode.

5. Conclusions

The results of this study provide insight into the potential application of hybrid processes implemented by combining electrocoagulation, zeolite addition, and ultrasound in wastewater treatment. The assistance of ultrasound in the simultaneous process (ECZ+US)

lowers the increase in pH, while a slight increase is observed in the two-step process (UC+Z - EC). However, it is noteworthy to point out that the electrode material's impact on pH always occurs in the following sequence: Zn > Fe > Al, regardless of the type of process. Even though the temperature rise in the ultrasonic bath was lower compared to the EC reactor, the ultrasound assistance contributed to the temperature rise. The temperature rise in the ultrasonic bath was also lower in the two-stage US+Z - EC due to the shorter exposure time (only 10 min of ultrasound). Looking at the type of electrode material, the temperature rise occurred in the following order: Zn > Al > Fe. The turbidity values fluctuated. The assistance of ultrasound led to a decrease in COD reduction for the Al and Fe electrodes, while a slight increase was observed for the Zn electrode in the two-stage US+Z - EC. As for the percentage of COD decrease, the highest values were obtained with the Al electrode (84.08–92.73%), followed by the Fe electrode (80.15–91.00%) and the Zn electrode (67.58–82.92). The final COD values for most of the hybrid process were slightly above the limits for discharge into the natural receiving water (125 mg O₂/L), while the values for ECZ with Al and Fe and ECZ+US with Fe were met. In the hybrid system with Fe electrodes, a lower voltage value was observed with simultaneous ECZ+US and two-stage US+Z - EC than with the ECZ. In the hybrid system with Al electrodes, a lower voltage value was observed with two-stage US+Z - EC compared to ECZ. Ultrasound assistance reduced the anode consumption for Al and Zn electrodes, while it caused a slight increase in anode consumption for Fe electrodes. The consumption of cathodes varied, but the consumption of aluminum cathodes was generally the highest. The assistance of ultrasound caused more damage to the anodes. The anode damage was more pronounced on the Al electrodes, with simultaneous ECZ+US, while the damage to the Fe and Zn electrodes was more pronounced with a two-stage hybrid process (US+Z - EC). The mass of EC sludge and saturated zeolite collected after each hybrid process varied between 10.0218 and 16.4454 g/L, depending on the type of hybrid process and electrode material, while the total amount of zeolite that could be regenerated was between 55 and 97%. The total amount of zeolite that could be regenerated was higher in the hybrid system, where a better turbidity reduction was achieved, and vice versa. In a hybrid system with Al and Fe electrodes, a good settling ability was achieved with ECZ and simultaneous ECZ+US (both settling curves were steep), while it was quite poor with the two-stage US+Z - EC (the settling curve was flattened). However, in a hybrid system with Zn electrodes, poor settling performance was achieved with all three hybrid processes.

Taguchi optimization shows that the electrode material and duration time have the greatest influence on COD reduction; mixing speed and process type on settling abilities; mixing speed and duration on voltage consumption; and electrode material and duration time on electrode mass consumed. The results show that ultrasound assistance does not, in general, have a positive effect on the quality of the wastewater treated regarding COD and turbidity. However, its application tends to decrease voltage and electrode consumption, thereby reducing the cost of the process.

Author Contributions: S.S.: conceptualization, writing—original draft, methodology, modeling, supervision, writing—review and editing. N.V.M. and L.V.: formal analysis, conceptualization, methodology, validation, writing—original draft, supervision, writing—review and editing. S.G.: formal analysis, investigation, writing—original draft, writing—review and editing. A.-M.M.: formal analysis, investigation. All authors have read and agreed to the published version of the manuscript.

Funding: The results of this paper are funded by institution funds of the Faculty of Chemistry and Technology University of Split, Croatia.

Data Availability Statement: The dataset analyzed in the current study is available from the corresponding author.

Conflicts of Interest: The authors declare that they have no competing interests.

References

1. Silva, J.A. Wastewater Treatment and Reuse for Sustainable Water Resources Management: A Systematic Literature Review. *Sustainability* **2023**, *15*, 10940. [[CrossRef](#)]
2. Wang, C.; Deng, S.-H.; You, N.; Bai, Y.; Jin, P.; Han, J. Pathways of wastewater treatment for resource recovery and energy minimization towards carbon neutrality and circular economy: Technological opinions. *Front. Environ. Chem.* **2023**, *4*, 1255092. [[CrossRef](#)]
3. Ang, W.L.; Mohammad, A.W. Chapter 9—Integrated and hybrid process technology. In *Sustainable Water and Wastewater Processing*; Galanakis, C.M., Agrafioti, E., Eds.; Elsevier: Amsterdam, The Netherlands, 2019; pp. 279–328. [[CrossRef](#)]
4. Fetyan, N.A.H.; Salem Attia, T.M. Water purification using ultrasound waves: Application and challenges. *Arab J. Basic Appl. Sci.* **2020**, *27*, 194–207. [[CrossRef](#)]
5. Wang, N.; Li, L.; Wang, K.; Huang, X.; Han, Y.; Ma, X.; Wang, M.; Lv, X.; Bai, X. Study and application status of ultrasound in organic wastewater treatment. *Sustainability* **2023**, *15*, 15524. [[CrossRef](#)]
6. Posavčić, H.; Vouk, D.; Halkijević, I. The effects of ultrasound and electrocoagulation on removal of manganese from wastewater. *Eng. Rev.* **2022**, *144*, 50–58. [[CrossRef](#)]
7. Zhang, M.; Zhang, Z.; Liu, S.; Peng, Y.; Chen, J.; Yoo Ki, S. Ultrasound-assisted electrochemical treatment for phenolic wastewater. *Ultrason. Sonochem.* **2020**, *65*, 105058. [[CrossRef](#)]
8. Sangave, P.C.; Pandit, A.B. Ultrasound pre-treatment for enhanced biodegradability of the distillery wastewater. *Ultrason. Sonochem.* **2004**, *11*, 197–203. [[CrossRef](#)]
9. Blume, T.; Neis, U. Improved wastewater disinfection by ultrasonic pre-treatment. *Ultrason. Sonochem.* **2004**, *11*, 333–336. [[CrossRef](#)]
10. Yin, X.; Lu, X.; Han, P.; Wang, Y. Ultrasonic treatment on activated sewage sludge from petro-plant for reduction. *Ultrasonics* **2006**, *44*, 397–399. [[CrossRef](#)]
11. Kyllonen, H.; Pirkonen, P.; Nystrom, M.; Nuortila-Jokinen, J.; Gronroos, A. Experimental aspects of ultra-sonically enhanced cross-flow membrane filtration of industrial wastewater. *Ultrason. Sonochem.* **2006**, *13*, 295–302. [[CrossRef](#)]
12. Emerick, T.; Vieira, J.L.; Silveira, M.H.L.; Joao, J.J. Ultrasound-assisted electrocoagulation process applied to the treatment and reuse of swine slaughterhouse wastewater. *J. Environ. Chem. Eng.* **2020**, *8*, 104308. [[CrossRef](#)]
13. Alnaimi, H.; Idan, I.J.; Al-Janabi, A.; Hashim, K.S.; Gkantou, M.; Zubaidi, S.L.; Kot, P.; Muradov, M. Ultrasonic-electrochemical treatment for effluents of concrete plants. *IOP Conf. Ser. Mater. Sci. Eng.* **2020**, *888*, 012063. [[CrossRef](#)]
14. Hassani, A.; Malhotra, M.; Karim, A.V.; Krishnan, S.; Nidheesh, P.V. Recent progress on ultrasound-assisted electrochemical processes: A review on mechanism, reactor strategies, and applications for wastewater treatment. *Environ. Res.* **2022**, *205*, 112463. [[CrossRef](#)]
15. Elazzouzi, M.; Haboubi, K.; Elyoubi, M.S. Electrocoagulation flocculation as a low-cost process for pollutants removal from urban wastewater. *Chem. Eng. Res. Des.* **2017**, *117*, 614–626. [[CrossRef](#)]
16. Zielinski, M.; Zielinska, M.; Debowski, M. Ammonium removal on zeolite modified by ultrasound. *Desalin. Water Treat.* **2015**, *57*, 8748–8753. [[CrossRef](#)]
17. Jahani, F.; Sadeghi, R.; Shakeri, M. Ultrasonic-assisted chemical modification of a natural clinoptilolite zeolite: Enhanced ammonium adsorption rate and resistance to disturbing ions. *J. Environ. Chem. Eng.* **2023**, *11*, 110354. [[CrossRef](#)]
18. Znak, Z.; Zin, O.; Mashtaler, A.; Korniy, S.; Sukhatskiy, Y.; Gogate, P.R.; Mnykh, R.; Thanekar, P. Improved modification of clinoptilolite with silver using ultrasonic radiation. *Ultrason. Sonochem.* **2021**, *73*, 105496. [[CrossRef](#)]
19. Erten-Kaya, Y.; Cakicioglu-Ozkan, F. Effect of ultrasound on the kinetics of cation exchange in NaX zeolite. *Ultrason. Sonochem.* **2012**, *19*, 701–706. [[CrossRef](#)]
20. Eaton, A.D.; Clesceri, L.S.; Rice, E.W.; Greenberg, A.E.; Franson, M.A.H. (Eds.) *Standard Methods for the Examination of Water and Wastewater*, 21st ed.; American Public Health Association (APHA): Cincinnati, OH, USA; American Water Works Association (AWWA): Washington, DC, USA; Water Environment Federation (WEF): Washington, DC, USA, 2005.
21. Svilović, S.; Vukojević Medvidović, N.; Vrsalović, L.; Kulić, A. Combining natural zeolite and electrocoagulation with different electrode materials—Electrode surface analysis and Taguchi optimization. *Appl. Surf. Sci. Adv.* **2022**, *12*, 100330. [[CrossRef](#)]
22. Vukojević Medvidović, N.; Vrsalović, L.; Svilović, S.; Magaš, K.; Jozić, D.; Čović, A. Electrocoagulation combined with synthetic zeolite—Does the size of zeolite particles matter? *Minerals* **2023**, *13*, 1141. [[CrossRef](#)]
23. Concha, A.F. Kynch Theory of Sedimentation. *Fluid Mech. Its Appl.* **2014**, *105*, 97–118. [[CrossRef](#)]
24. Hunter, R.J. *Foundations of Colloid Science*; Oxford University Press: New York, NY, USA, 1989.
25. Russel, W.B.; Saville, D.A.; Schowalter, W.R. *Colloidal Dispersions*; Cambridge University Press: Cambridge, UK, 1989.
26. Chen, G. Electrochemical technologies in wastewater treatment. *Sep. Purif. Technol.* **2004**, *38*, 11–41. [[CrossRef](#)]
27. Mouedhen, G.; Feki, M.; De Petris Wery, M.; Ayedi, H.F. Behavior of aluminum electrodes in electrocoagulation process. *J. Hazard. Mater.* **2008**, *150*, 124–135. [[CrossRef](#)] [[PubMed](#)]
28. Vargel, C.; Jacques, M.; Schmidt, M.P. *Corrosion of Aluminium*; Elsevier: Amsterdam, The Netherlands, 2004.
29. Tao, J. Surface Composition and Corrosion Behavior of an Al-Cu Alloy. Ph.D. Thesis, Université Pierre et Marie Curie—Paris VI, Paris, France, 2016.
30. Krezel, A.; Maret, W. The biological chemistry of zinc ions. *Arch. Biochem. Biophys.* **2016**, *611*, 3–19. [[CrossRef](#)] [[PubMed](#)]

31. Arumuganathan, T.; Srinivasaro, A.; Kumar, T.V.; Das, S.K. Two different zinc(II)-aqua complexes held up by a metal-oxide based support: Synthesis, crystal structure and catalytic activity of $[\text{HMTAH}]_2[\{\text{Zn}(\text{H}_2\text{O})_5\}\{\text{Zn}(\text{H}_2\text{O})_4\}\{\text{Mo}_7\text{O}_{24}\}] \times 2\text{H}_2\text{O}$ (HMTAH = protonated hexamethylenetetramine). *J. Chem. Sci.* **2008**, *120*, 95–103. [[CrossRef](#)]
32. Beverskog, B.; Puigdomenech, I. Revised Pourbaix diagrams for iron at 25–300 °C. *Corros. Sci.* **1996**, *38*, 2121–2135. [[CrossRef](#)]
33. Asgharian, F.; Khosravi-Nikou, M.; Anvaripour, B.; Danaee, I. Electrocoagulation and ultrasonic removal of humic acid from wastewater. *Environ. Prog. Sust. Energy.* **2017**, *36*, 822–829. [[CrossRef](#)]
34. Croatian Regulation on Emission Limits Values in Wastewater, NN 26/2020. Available online: https://narodne-novine.nn.hr/clanci/sluzbeni/2020_03_26_622.html (accessed on 15 April 2024). (In Croatian).
35. Cai, Y.; Li, J.; Qu, G.; Ren, N.; Zou, H.; Hu, Y.; Qiu, W. Research on dynamics and mechanism of treatment on phenol simulated wastewater by the ultrasound cooperated electro-assisted micro-electrolysis. *Water Environ. Res.* **2021**, *93*, 1243–1253. [[CrossRef](#)]
36. De Morais, N.L.P.A.; Brett, C.M.A. Influence of power ultrasound on the corrosion of aluminium and high speed steel. *J. Appl. Electrochem.* **2002**, *32*, 653–660. [[CrossRef](#)]
37. Doche, M.L.; Hihn, J.Y.; Mandroyan, A.; Viennet, R.; Touyeras, F. Influence of ultrasound power and frequency upon corrosion kinetics of zinc in saline media. *Ultrason. Sonochem.* **2003**, *10*, 357–362. [[CrossRef](#)]
38. Vukojević Medvidović, N.; Vrsalović, L.; Svilović, S.; Bilušić, A.; Jozić, D. Electrocoagulation treatment of compost leachate using aluminium alloy, carbon steel and zinc anode. *Appl. Surf. Sci. Adv.* **2023**, *15*, 100404. [[CrossRef](#)]
39. Marlow, B.J.; Rowell, R.L. Sedimentation potential in aqueous electrolytes. *Langmuir* **1985**, *1*, 83–90. [[CrossRef](#)]
40. Hirakawa, H. Measurement of sedimentation potential and its application to the determination of individual ionic partial molar volumes. *J. Phys. Chem.* **1987**, *91*, 3452–3456. [[CrossRef](#)]
41. Svilović, S.; Mužek, M.N.; Vučenović, P.; Nuić, I. Taguchi design of optimum process parameters for sorption of copper ions using different sorbents. *Water Sci. Technol.* **2019**, *80*, 98–108. [[CrossRef](#)]
42. Graça, N.S.; Rodrigues, A.E. The combined implementation of electrocoagulation and adsorption process for the treatment of the wastewaters. *Clean Technol.* **2022**, *4*, 1020–1053. [[CrossRef](#)]

Disclaimer/Publisher’s Note: The statements, opinions and data contained in all publications are solely those of the individual author(s) and contributor(s) and not of MDPI and/or the editor(s). MDPI and/or the editor(s) disclaim responsibility for any injury to people or property resulting from any ideas, methods, instructions or products referred to in the content.